Journal of Alloys and Compounds 515 (2012) 12–15

Contents lists available at SciVerse ScienceDirect

Journal of Alloys and Compounds

journal homepage: www.elsevier.com/locate/jallcom

Letter

Study of electronic and magnetic properties of vacuum annealed Cr doped ZnO

Asmita Singhal*

Birla Institute of Technology, Mesra (Jaipur Extension Centre), Jaipur 302017, India

ARTICLE INFO

Article history:
Received 1 June 2011
Received in revised form
17 November 2011
Accepted 22 November 2011
Available online 1 December 2011

Keywords:
Dilute magnetic semiconductors
X-ray photoelectron spectroscopy
Magnetic properties

ABSTRACT

Influence of Cr doping (5%) in ZnO lattice has been investigated in terms of modifications in electronic properties, evolution of defects and exploring their possible relationship with magnetic properties, using SQUID magnetometry and X-ray photoelectron spectroscopy (XPS). The Cr doping drives the diamagnetic ZnO host to a paramagnetic state, however, its post annealing in vacuum induces room temperature ferromagnetism (RTFM) in it that disappears by re-heating it in air. The findings infer a reversible ferromagnetic ordering in the Cr doped ZnO matrix. The XPS results indicate trivalent state of the Cr ions in the as-synthesized sample which tend to reduce to bivalency upon its vacuum annealing and also the evolution of oxygen vacancy defects have clearly been observed. The results indicate a close relationship of oxygen vacancies with the induced ferromagnetism.

1. Introduction

The ZnO based magnetic semiconductors have attracted immense research attention due to their promising versatile applications e.g. in spintronics, optoelectronics, and piezoelectric materials. Dietl et al. [1], based on local spin density approximation, predicted the possibility of occurrence of high T_C ferromagnetism in *p*-doped ZnO and GaN. Based on the band calculations, Sato and Katayama-Yoshida [2] had also made the similar theoretical predictions. Subsequently, various experiments on ZnO doped by 3*d* transition metal ions in different forms were carried out to confirm the predictions of RTFM. Unfortunately, the experimental results could not reach definite conclusions owing to controversial reports as the findings differ widely [3–5] in this regard. The same material system has been reported to display ferromagnetic, paramagnetic or spin glass behavior, depending on the sample preparation parameters. The possibilities of precipitation of secondary phases or the dopants into metallic clusters have also not been ruled out. Their magnetic properties are reported to be sensitive to the preparation methods and the resulting structure. Despite a lot of efforts, the mechanism of ferromagnetic ordering in these systems is far from clear as yet.

The structural, optical and magnetic properties of different doped ZnO systems in different forms e.g. the polycrystalline, thin films and nano-crystals have been reported in the most recent studies [6–11]. Tan et al. [6] studied the polycrystalline Eu-doped ZnO films. They showed that Eu ions substitute for the Zn^{2+} ions in the ZnO lattice. The films show a clear RTFM which is attributed to the intrinsic property of the Eu-doped films. The bound-magnetic-polaron is reported to be responsible for the ferromagnetism. Liu et al. [7] synthesized the $Zn_{1-x}Cr_xO$ ($0 \le x \le 0.08$) nanoparticles by sol–gel method and characterized them using energy dispersive spectroscopy, X-ray diffraction, transmission electron microscope, X-ray photoelectron spectroscopy and X-ray absorption fine structure. The nano particles were reported to show good high-T_C ferromagnetism. They concluded that the observed ferromagnetism is an intrinsic property of the Cr-doped ZnO nanoparticles. Arshad et al. [8] studied the Effect of Co substitution on the structural and optical properties of ZnO nanoparticles synthesized by sol–gel route and characterized those using different techniques. They reported an increase in the band gap and a decrease in the particle size as a function of increase in the Co concentration.

The $Zn_{1-x}Co_xO$ and $Zn_{1-x}Mn_xO$ systems have most widely been investigated in this regard. The ferromagnetism is observed in them [12–15], while the discrepancies continue in whether the ferromagnetism is intrinsic in nature [16–19] or due to spurious signals from the ferromagnetic impurities. By comparison, a lesser attention has been paid to Cr- and Ni-doped systems [20,21]. In this article, I am presenting the investigations of structural, electronic and magnetic properties of a 5% Cr doped ZnO system.

2. Experimental details

Appropriate amounts of Zn and Cr oxide powders (purity ≥ 99.999%) were mixed and ground for 14 h, followed by calcination at 650 °C for 12 h. The mixture was re-ground and heated at 900 °C for 12 h. The pellets of 8 mm diameter were prepared and sintered at 500 °C for 18 h. The sample powder was annealed in vacuum (pressure 10^{-8} bar, temperature 700 °C, duration 40 h) and then re-heated in air (temperature 700 °C, duration 30 h). The crystal structures were determined by analyzing the X-ray diffraction (XRD) patterns using Rietveld refinement program

* Tel.: +91 141 2761545.
E-mail address: asmitasinghal17@gmail.com

0925-8388/$ – see front matter © 2011 Elsevier B.V. All rights reserved.
doi:10.1016/j.jallcom.2011.11.103

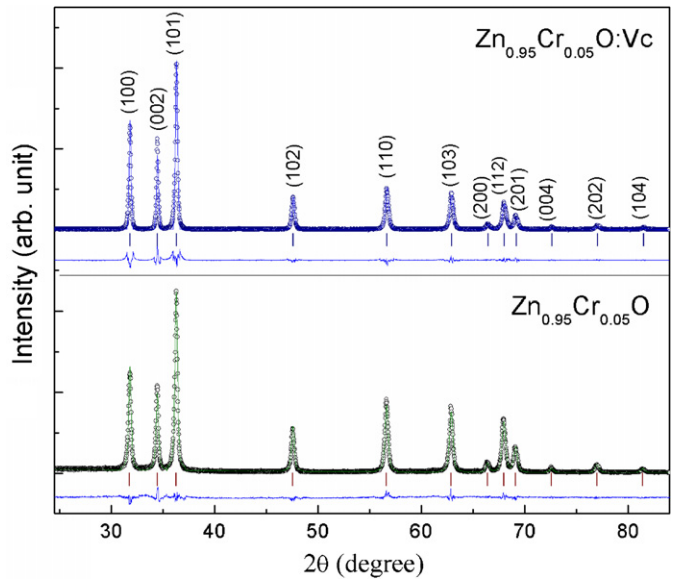

Fig. 1. The Rietveld fitted and indexed XRD patterns for $Zn_{0.95}Cr_{0.05}O$ and $Zn_{0.95}Cr_{0.05}O$:Vc.

FULLPROF [22]. The DC magnetization measurements were performed using SQUID magnetometer. The core level XPS spectra were measured using Al K_α radiation, maintaining the vacuum of the order of $\sim 5 \times 10^{-10}$ Torr in the sample chamber.

3. Experimental results

3.1. Structural characterization by XRD

Fig. 1 shows the indexed XRD patterns for the as-synthesized sample $Zn_{0.95}Cr_{0.05}O$ and the vacuum annealed sample $Zn_{0.95}Cr_{0.05}O$:Vc. Rietveld refinement of the patterns, demonstrates that all the Bragg peaks are indexed in the wurtzite structure (space group P63mc: No. 186, $z = 2$) with no additional peaks from any secondary phase. The cell parameters of $Zn_{0.95}Cr_{0.05}O$ are slightly smaller than the pure ZnO ($a = 3.2488(4)$ Å, $c = 5.2069(5)$ Å) which can be assigned to a smaller ionic radius of Cr^{3+} (0.52 Å) than that of Zn^{2+} (0.60 Å). These cell parameters are, however, slightly smaller than those reported by Paul Joseph et al. [20] for nano-crystalline sample $Zn_{0.95}Cr_{0.05}O$, prepared by chemical co-precipitation ($a = b = 3.260$ Å and $c = 5.217$ Å).

3.2. Magnetization results

The pure ZnO is diamagnetic (Fig. 2a) while the sample $Zn_{0.95}Cr_{0.05}O$ is paramagnetic (Fig. 2b), however, upon vacuum annealing ($Zn_{0.95}Cr_{0.05}O$:Vc) it shows a room temperature ferromagnetism (saturation magnetization Ms ~0.036 emu/g, and coercive field Hc ~197 Oe) (Fig. 2c). The induced RTFM disappears when the vacuum annealed sample is re-heated in air (Fig. 2b). These results demonstrate the evidence of an "*on*" and "*off*" switch action, identical to that reported in transition metal doped oxide systems of ZnO, TiO_2, In_2O_3 and CeO_2 [13,14,19,23–25]. It is important to mention that the similar vacuum annealing of non-doped ZnO could not induce any RTFM in it. The M–T curve measured for $Zn_{0.95}Cr_{0.05}O$:Vc at $H = 1$ T demonstrates its T_C to be ~500 K (Fig. 2d).

3.3. X-ray photoelectron spectroscopy results

Before measuring the final spectra the sample surfaces were scraped uniformly *in situ* until the spectral feature coming from the surface (C 1*s* peak) got minimized. The binding energies were corrected with reference to the C1*s* peak (284.6 eV).

3.3.1. Zinc 2p XPS spectra

The Zn *2p* XPS spectra for ZnO, $Zn_{0.95}Cr_{0.05}O$ and $Zn_{0.95}Cr_{0.05}O$:Vc samples are shown in Fig. 3a. All the spectra show sharp and symmetric single peaks at ~1022.5 eV and ~1046 eV, corresponding to the Zn 2*p*3/2 and 2*p*1/2 states, respectively. These peak positions match closely with the standard energy values of ZnO [14,24,26,27], indicating that Zn atoms are in +2 valence state and the Cr doping and vacuum annealing do not change their valence states. The intensity under the *2p* peaks slightly lowers upon doping, confirming that the Cr ions substitute the Zn site within the wurtzite structure.

3.3.2. Chromium 2p XPS spectra

Fig. 3b displays the Cr *2p* XPS spectrum for sample $Zn_{0.95}Cr_{0.05}O$. The spectrum shows the peaks Cr 2*p*3/2 and 2*p*1/2 at ~576.8 eV and ~585.8 eV, respectively. The Cr 2*p*3/2 position located at 576.8 eV is very close to the position of Cr 2*p*3/2 in Cr_2O_3 that occurs at ~576.7 eV [28–30]. The position of the Cr 2*p*3/2 peak is significantly away from that of Cr metal (~574.2 eV) which rules out the presence of Cr clusters in our Cr-doped sample. Also the peak Cr 2*p*3/2 lies on much higher energy side of the Cr^{2+} state (the later occurs at ~576 eV). Therefore, the peak position of Cr 2*p*3/2 can be assigned to the Cr^{3+} state since it matches well with the binding energy of Cr^{3+} valence state [28–30]. Upon vacuum annealing the sample the Cr 2*p*3/2 peak shifts to lower energy which could be assigned to reduction of Cr^{3+} state to Cr^{2+}, owing to a possible Cr (*3d*)—O (*2p*) charge transfer process. Interestingly, upon air re-heating the annealed samples, the peak position is shifted back to the original position.

The intensity of the peak Cr 2*p*3/2 is much higher than the Cr 2*p*1/2. It is known that the 2*p* level splits into two sub-levels 2*p*3/2 and 2*p*1/2 and the ratio of occupancy in them is 2:1. Naturally, the intensity of photoelectron signal emerging from the 2*p*3/2 state is much more than that from the 2*p*1/2. Strangely, the spectrum shown by Liu et al. [30] shows that the intensity of 2*p*3/2 signal is almost half than that of 2*p*1/2. Even the spectra in Refs. [26,28] show that the Cr spectrum is very much similar to that presented here.

3.3.3. Oxygen 1s spectra

The O 1*s* spectra which were asymmetric in shape, were fitted with three Gaussians (Fig. 3c) to separate out the bulk O_2 content. The main peak at ~531.5 eV belongs to the bulk O_2 while the small structures on the higher energy side arise due to surface impurities [14,16,23]. The bulk O_2 peaks are compared in Fig. 3d. There is a notable deficiency in the bulk O_2 in $Zn_{0.95}Cr_{0.05}O$:Vc than that in the as-synthesized sample $Zn_{0.95}Cr_{0.05}O$ which is a clear indication of creation of the oxygen vacancies. The oxygen vacancies seems to be created in the lattice in order to conserve the total charge in the sample, modified as a consequence of reduction of Cr^{3+} ions to the Cr^{2+} state upon its vacuum annealing (discussed above). Interestingly, upon re-heating the vacuum annealed sample ($Zn_{0.95}Cr_{0.05}O$:Vc) in air, the bulk O_2 content is almost recovered.

4. Discussion

These results are quantitatively summarized in Fig. 4. Fig. 4a shows the M_S at field $H = 1$ T after the different annealing stages (*viz.*1, 2, and 3) indicating the samples: as-synthesized, annealed in vacuum and re-heated in air, respectively. The M_S decreases and then increases when it passes through these stages, showing a reversible cycle of magnetization process. Fig. 4b shows that the O_2 contents in these stages first increases and then decreases. The

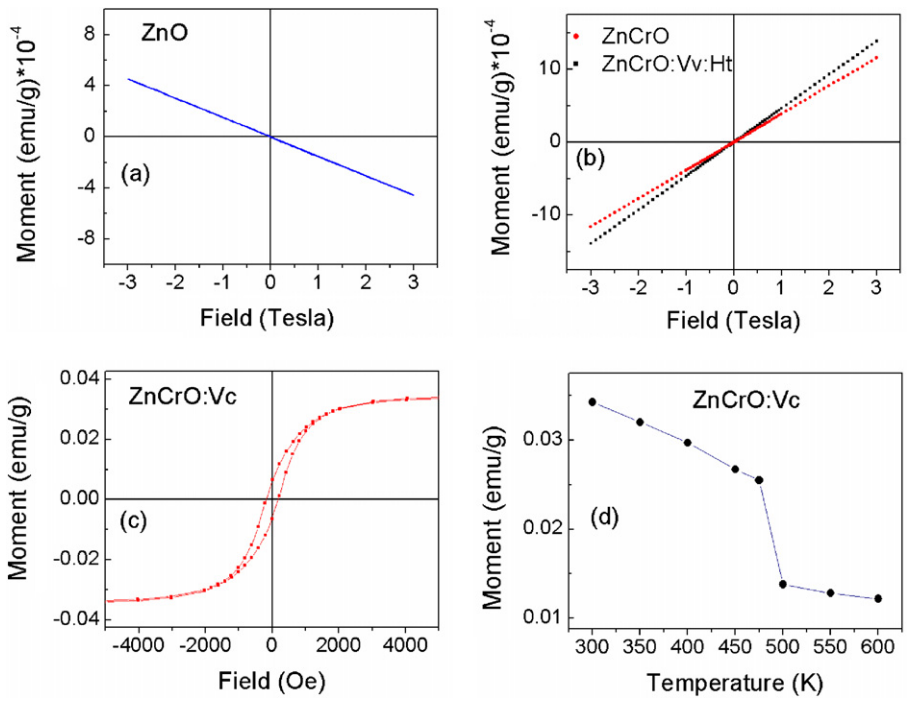

Fig. 2. M–H curves at 300 K for (a). ZnO (b). $Zn_{0.95}Cr_{0.05}O$ (c). $Zn_{0.95}Cr_{0.05}O$:Vc (d). M–T graph for $Zn_{0.95}Cr_{0.05}O$:Vc. The M–H curves for re-heated $Zn_{0.95}Cr_{0.05}O$:Vc:Ht are shown in part figure b.

O_2 content in the doped samples has been estimated with respect to the pure ZnO sample taken as unity. The O_2 deficiency indicates the creation of O vacancies in the doped samples. These results establish that the magnetization and demagnetization process are reversible with regard to oxygen vacancies in agreement with Refs. [13,14,19,23–25].

The origin of FM in TM-doped ZnO samples is still undetermined. There might be two possible causes for the ferromagnetism in $Zn_{0.95}Cr_{0.05}O$:Vc (i) clustering of metallic Cr ions or the secondary magnetic phases and/or (ii) an intrinsic ferromagnetism. But the Rietveld analysis of XRD patterns and the XPS findings rule out any secondary phase formation in our samples, nevertheless, the unidentified traces of various chromium oxides are unlikely sources of ferromagnetism due to the following facts: the bulk Cr_2O_3 is anti-ferromagnetic insulator with $T_N \sim 307$ K [31]. The CrO_2 metallic and ferromagnetic, however, it has a $T_C \sim 391$ K [32]. The α-Cr_2O_5

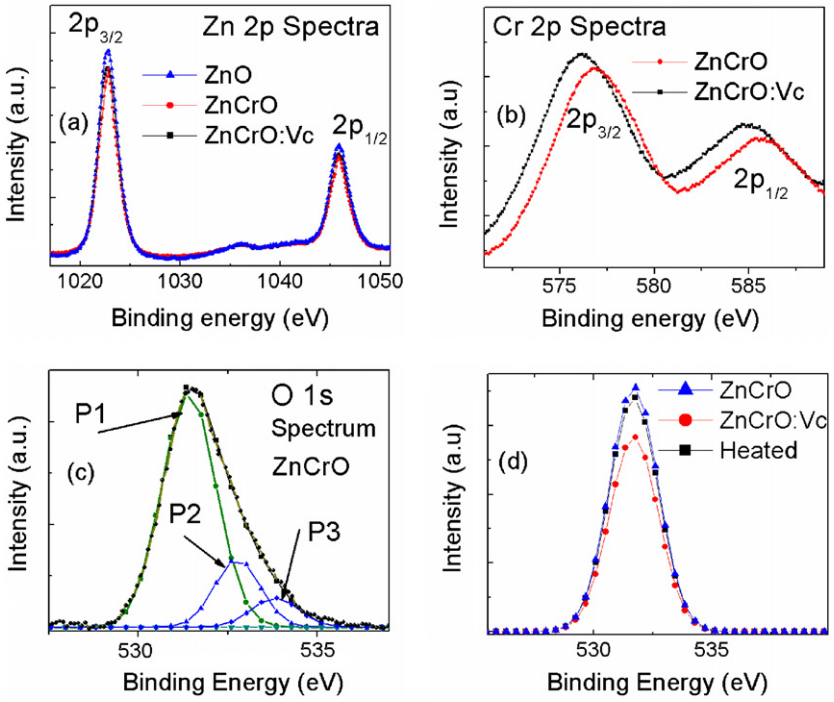

Fig. 3. (a) Zn *2p* XPS spectra of ZnO, $Zn_{0.95}Cr_{0.05}O$ and $Zn_{0.95}Cr_{0.05}O$:Vc (b). Cr *2p* XPS spectra of $Zn_{0.95}Cr_{0.05}O$ and $Zn_{0.95}Cr_{0.05}O$:Vc (c). Oxygen 1*s* XPS spectra for $Zn_{0.95}Cr_{0.05}O$ with Gaussian fits (d). Oxygen bulk peaks for $Zn_{0.95}Cr_{0.05}O$, $Zn_{0.95}Cr_{0.05}O$:Vc and $Zn_{0.95}Cr_{0.05}O$:Vc:Ht.

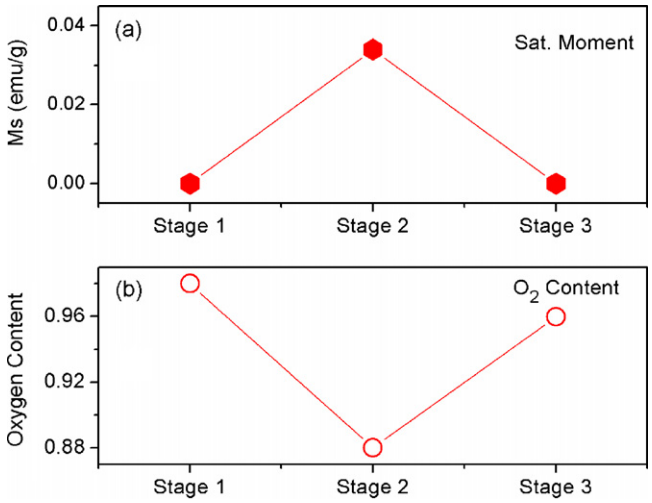

Fig. 4. The saturation magnetization (M_S) at $H = 1$ T and the oxygen content in the samples relative to pure ZnO. The stages 1, 2, 3, indicate the samples $Zn_{0.95}Cr_{0.05}O$: as-synthesized, annealed in vacuum and re-annealed in air, respectively.

reported to be produced by heating chromium oxides in vacuum has a $T_C \sim 140$ K [33]. Since $Zn_{0.95}Cr_{0.05}O$:Vc has a much higher T_C (~500 K) these possibilities can be kept aside. The other oxides are paramagnetic in nature.

The Ruderman, Kittel, Kasuya and Yosida (RKKY) interaction is one amongst the others which has been used to explain the formation of magnetic phases in DMS materials. This is based on the concentration of free carriers apart from the concentration of magnetic ions. The ZnO is a native n-type material due to oxygen vacancies and zinc interstitials. Hence, the concentration of free electrons has been proposed to play a major role in stabilizing the magnetic phase. Consequently, a ferromagnetic phase may be favored at higher electron concentrations at room temperature because their mean free path is reduced limiting the interaction to the few relatively stronger and ferromagnetically ordered nearest neighbors [20].

However, in present case, the mixed valence of the doped Cr ions has been confirmed which suggests the inclusion of double exchange mechanism between d states of TM elements [34] as an important factor in the observed ferromagnetism. In addition, several groups have found that the point defects play crucial roles in inducing ferromagnetism in the ZnO-based systems [35,36]. Zhuge et al. [37] found that the magnetization in their Cr-doped ZnO films is correlated to vacancies at the Zn sites (V_{Zn}). Hong et al. [38] have ascribed the FM in Cr-doped ZnO films to the oxygen vacancies (V_O). The present findings support the later viewpoint as the V_O's have clearly been observed in the ferromagnetic sample $Zn_{0.95}Cr_{0.05}O$:Vc which disappear when the sample returns to paramagnetic state upon re-heating it in air. Based on these observations I assert that the observed ferromagnetism in $Zn_{0.95}Cr_{0.05}O$:Vc might originate following the exchange interaction between the Cr^{2+} ions mediated by the O vacancies, emerged upon vacuum annealing owing to the Cr (*3d*)—O (*2p*) charge transfer. More detailed work is essential in order to understand the magnetic behaviors of these materials.

5. Conclusions

A paramagnetic behavior is observed in the as-synthesized $Zn_{0.95}Cr_{0.05}O$, however, upon vacuum annealing, it showed ferromagnetic ordering followed by creation of oxygen vacancies. Annealing of pure ZnO in identical atmospheres gave negative results in this regard inferring that presence of Cr ions in ZnO matrix are crucial for creation of the oxygen vacancies and inducing the room temperature ferromagnetism. Interestingly, the induced magnetism disappears upon re-heating the annealed samples in air. It is concluded that the observed ferromagnetism in $Zn_{0.95}Cr_{0.05}O$:Vc might originate following the exchange interaction between Cr^{2+} ions mediated by O vacancies, emerged upon vacuum annealing owing to the Cr (*3d*)—O (*2p*) charge transfer.

References

[1] T. Dietl, H. Ohno, F. Matsukura, J. Cibert, D. Ferrand, Science 287 (2000) 1019–1022.
[2] K. Sato, H. Katayama-Yoshida, Jpn. J. Appl. Phys. 39 (2000) L555.
[3] R. Bhargava, P.K. Sharma, A.K. Chawla, S. Kumar, R. Chandra, A.C. Pandey, N. Kumar, Mater. Chem. Phys. 125 (2011) 664–671.
[4] A.E. Kandjani, M.F. Tabriz, O.M. Moradi, H.R. Mehr, S.A. Kandjani, M.R. Vaezi, J. Alloys Compd. 509 (2011) 7854–7860.
[5] N. Al-Hardan, M.J. Abdullah, A. Abdul Aziz, Appl. Surf. Sci. 257 (2011) 8993–8997.
[6] Y. Tan, Z. Fang, W. Chen, P. He, J. Alloys Compd. 509 (2011) 6321–6324.
[7] Y. Liu, Y. Yang, J. Yang, Q. Guan, H. Liu, L. Yang, Y. Zhang, Y. Wang, M. Wei, X. Liu, L. Fei, X. Cheng, J. Solid State Chem. 184 (2011) 1273–1278.
[8] M. Arshad, A. Azam, A.S. Ahmed, S. Mollah, A.H. Naqvi, J. Alloys Compd. 509 (2011) 8378–8381.
[9] F. Cai, L. Zhu, H. He, J. Li, Y. Yang, X. Chen, Z. Ye, J. Alloys Compd. 509 (2011) 316–320.
[10] X. Pang, J. Zhang, K. Gao, A.A. Volinsky, Mater. Lett. 65 (2011) 2728–2730.
[11] X. Wang, L. Zhu, L. Zhang, J. Jiang, Z. Yang, Z. Ye, B. He, J. Alloys Compd. 509 (2011) 3282–3285.
[12] H.J. Lee, S.Y. Jeong, C.R. Cho, C.H. Park, Appl. Phys. Lett. 81 (2002) 4020–4022.
[13] R.K. Singhal, A.Samariya, S. Kumar, Y.T. Xing, U.P. Deshpande, T. Shripathi, S.N. Dolia, E. Saitovitch, Phys. Status Solidi (A) 207 (2010) 2373–2386.
[14] R.K. Singhal, A. Samariya, Y.T. Xing, S. Kumar, S.N. Dolia, T. Shripathi, U.P. Deshpande, E. Saitovitch, J. Alloys Compd. 496 (2010) 324–330.
[15] A. Singhal, J. Alloys Compd. 507 (2010) 312–316.
[16] X.M. Cheng, C.L. Chien, J. Appl. Phys. 93 (2003) 7876.
[17] J.H. Kim, H. Kim, D. Kim, S.G. Yoon, W.K. Choo, Solid State Commun. 131 (2004) 677–680.
[18] J.H. Park, M.G. Kim, H.M. Jang, S. Ryu, Y.M. Kim, Appl. Phys. Lett. 84 (2004) 1338.
[19] R.K. Singhal, A. Samariya, S. Kumar, Y.T. Xing, D.C. Jain, S.N. Dolia, U.P. Deshpande, T. Shripathi, E. Saitovitch, J. Appl. Phys. 107 (2010) 113916.
[20] D. Paul Joseph, S. Naveenkumar, N. Sivakumar, C. Venkateswaran, Mater. Chem. Phys. 97 (2006) 188–192.
[21] D. Paul Joseph, S. Ayyappan, C. Venkateswaran, J. Alloys Compd. 415 (2006) 225–228.
[22] J. Rodriguez-Carvajal, FULLPROF Version 3.0.0, Lab. Leon Brillouin, (CEA-CNRS), 2003.
[23] R.K. Singhal, P. Kumari, A. Samariya, S. Kumar, S.C. Sharma, Y.T. Xing, E. Saitovitch, Appl. Phys. Lett. 97 (2010) 172503.
[24] A. Samariya, R.K. Singhal, S. Kumar, Y.T. Xing, M. Alzamora, S.N. Dolia, U.P. Deshpande, T. Shripathi, E. Saitovitch, Mater. Chem. Phys. 123 (2010) 678–684.
[25] A. Samariya, R.K. Singhal, S. Kumar, Y.T. Xing, S.C. Sharma, P. Kumari, D.C.##S.N. Jain, Dolia U.P. Deshpande, T. Shripathi, E. Saitovitch, Appl. Surf. Sci. 257 (2010) 585–590.
[26] R.K. Singhal, Appl. Surf. Sci. 257 (2010) 1808–1809.
[27] C.D. Wagner, W.M. Riggs, L.E. Davis, J.F. Moulder, G.E. Muilenberg, Handbook of X-ray Photoelectron Spectroscopy, Perkin Elmer, Eden Prairie, 1979, pp. 80–84.
[28] B. Wang, J. Iqbal, X. Shan, G. Huang, H. Fu, R. Yu, D. Yu, Mater. Chem. Phys. 113 (2009) 103–106.
[29] A.B. Gaspar, C.A.C. Perez, L.C. Dieguez, Appl. Surf. Sci. 252 (2005) 939–949.
[30] Y. Liu, J. Yang, Q. Guan, L. Yang, H. Liu, Y. Zhang, Y. Wang, D. Wang, J. Lang, Y. Yang, L. Fei, M. Wei, Appl. Surf. Sci. 256 (2010) 3559–3562.
[31] A.F. Holleman, E. Wiberg, Inorganic Chemistry, Academic Press, New York, 2001.
[32] M. Rabe, J. Dreben, D. Dahmen, J. Pommer, H. Stahl, U. RuKdiger, G. GuKntherodt, S. Senz, D. Hesse, J. Magn. Magn. Mater. 211 (2000) 314–319.
[33] T.A. Hewston, B.L. Chamberland, J. Magn. Magn. Mater. 43 (1984) 89–95.
[34] P.M. Krstajic, F.M. Peeters, V.A. Ivanov, V. Fleurov, K. Kikoin, Phys. Rev. B 70 (2004) 195215.
[35] G.Z. Xing, J.B. Yi, J.G. Tao, T. Liu, L.M. Wong, Z. Zhang, G.P. Li, S.J. Wang, J. Ding, T.C. Sum, C.H.A. Huan, T. Wu, Adv. Mater. 20 (2008) 3521.
[36] G.Z. Xing, J.B. Yi, D.D. Wang, L. Liao, T. Yu, Z.X. Shen, C.H.A. Huan, T.C. Sum, J. Ding, T. Wu, Phys. Rev. B 79 (2009) 174406.
[37] L.J. Zhuge, X.M. Wu, Z.F. Wu, X.M. Chen, Y.D. Meng, Scr. Mater. 60 (2009) 214–217.
[38] N.H. Hong, J. Sakai, N.T. Huong, N. Poirot, A. Ruyter, Phys. Rev. B 72 (2005) 045336.